current issues in molecular biology

MDPI

Article

Trigonella foenum-graecum L. Extract Activates a Gβγ/PLC-Dependent Pathway to Promote GLP-1 Secretion and Improve Glucose Metabolism in T2DM

Hongjuan Niu [1,2,3,4,5,6,†], Rongfei Yao [6,†], Luxuan Chi [6], Yang Niu [6], Heng Pan [1,2,3,4,5], Jiaqi Xu [1,2,3,4,5,*] and Zongran Pang [6,*]

[1] State Key Laboratory of Female Fertility Promotion, Center for Reproductive Medicine, Department of Obstetrics and Gynecology, Peking University Third Hospital, Beijing 100191, China; nhj1113@bjmu.edu.cn (H.N.); hep2007@bjmu.edu.cn (H.P.)
[2] Key Laboratory of Assisted Reproduction in Peking University, Ministry of Education, Beijing 100191, China
[3] Beijing Key Laboratory of Collaborative Innovation in Frontier Technologies for Population Quality, Beijing 100191, China
[4] National Clinical Research Center for Obstetrics and Gynecology, Peking University Third Hospital, Beijing 100191, China
[5] National Clinical Key Specialty Construction Program, Beijing 100191, China
[6] School of Pharmacy, Minzu University of China, Beijing 100081, China; 20400224@muc.edu.cn (R.Y.); c18379973052@163.com (L.C.); n15233121472@163.com (Y.N.)
* Correspondence: xujiaqi1001@sina.com (J.X.); zrpang@163.com (Z.P.)
† These authors contributed equally to this work.

Abstract

Objective: *Trigonella foenum-graecum* L. (fenugreek) is a characteristic bitter herb traditionally prepared as decoctions to treat diabetes. This study aimed to elucidate whether the traditional "bitter" property of fenugreek aqueous extract (FGE) exerts anti-diabetic effects by targeting the intestinal bitter taste receptor Tas2r138 (the murine functional ortholog of human TAS2R38) and modulating the GLP-1-mediated entero-pancreatic axis. **Methods:** Dried fenugreek seeds were extracted with distilled water and lyophilized. Following standardization via absolute quantitative HPLC, FGE was orally administered to type 2 diabetic (T2DM) mice at doses of 0.26 and 0.52 g/kg/day for four weeks. The underlying mechanisms were investigated using UPLC-MS/MS, network pharmacology, molecular dynamics (MD) simulations, and in vitro assays in STC-1 enteroendocrine cells. **Results:** FGE significantly reduced blood glucose levels and ameliorated hyperphagia, insulin resistance, and dyslipidemia in the T2DM model, exhibiting efficacy comparable to the positive control, metformin. Notably, FGE markedly elevated systemic total GLP-1 levels and restored pancreatic islet architecture. Mechanistically, FGE upregulated intestinal *Tas2r138* expression and activated the PLCβ2/TRPM5 signaling pathway. HPLC quantification identified trigonelline (15.1 mg/g extract) as the primary bitter constituent, displaying favorable predicted docking interactions with the human TAS2R38 receptor. In STC-1 cells, trigonelline directly stimulated intracellular Ca^{2+} flux and GLP-1 secretion, effects that were significantly attenuated by Gβγ and PLC inhibitors, suggesting the involvement of a Gq-coupled GPCR signaling pathway. **Conclusions:** These findings provide a scientific rationale for the traditional use of fenugreek in metabolic disorders, demonstrating that FGE restores glucose and lipid homeostasis via a trigonelline-driven, Gβγ/PLC-dependent pathway, which is consistent with the modulation of the intestinal Tas2r138-GLP-1-pancreatic insulin axis.

Keywords: *Trigonella foenum-graecum* L.; type 2 diabetes mellitus; Tas2r138; GLP-1; gut-pancreas axis

Check for updates

Received: 21 July 2026
Revised: 23 September 2026
Accepted: 5 October 2026
Published: 4 November 2026

Copyright: © 2026 by the authors. Licensee MDPI, Basel, Switzerland. This article is an open access article distributed under the terms and conditions of the Creative Commons Attribution (CC BY) license.

1. Introduction

Diabetes mellitus (DM) represents one of the most pressing global health challenges, imposing a substantial socio-economic burden on healthcare systems worldwide. Epidemiological data indicate that China harbors the largest population of adults with diabetes, highlighting the urgent need for effective therapeutic strategies. Among all forms of diabetes, type 2 diabetes mellitus (T2DM) accounts for approximately 90–95% of cases and is characterized by chronic hyperglycemia resulting from insulin resistance (IR) and impaired pancreatic β-cell function [1]. The pathogenesis of T2DM is multifactorial and involves complex interactions among genetic predisposition, environmental factors, and metabolic dysregulation, ultimately leading to β-cell dysfunction and systemic IR [2,3]. Current clinical management of T2DM relies mainly on pharmacological therapies combined with dietary and lifestyle interventions.

Increasing evidence indicates that the gastrointestinal tract functions as an important metabolic regulatory organ through the secretion of enteroendocrine hormones. Among these hormones, glucagon-like peptide-1 (GLP-1), primarily secreted by enteroendocrine L-cells located in the ileum and colon, plays a central role in maintaining glucose homeostasis. GLP-1 enhances glucose-dependent insulin secretion from pancreatic β-cells, promotes β-cell proliferation and survival, and suppresses glucagon secretion. These physiological effects form the basis for the widespread clinical use of GLP-1 receptor (GLP-1R) agonists and dipeptidyl peptidase-4 (DPP-4) inhibitors in the treatment of T2DM [4,5]. However, the exogenous injectable nature of GLP-1 analogues and the associated continuous, supraphysiological GLP-1 levels frequently cause adverse gastrointestinal effects, such as severe nausea and vomiting [6,7]. Consequently, stimulating the endogenous release of GLP-1 via intestinal nutrient sensors using oral natural compounds presents a highly promising and physiologically tolerable alternative therapeutic paradigm.

Recent studies have revealed that bitter taste receptors (TAS2Rs), originally discovered in the oral cavity, are widely expressed in extraoral tissues including the gastrointestinal tract. In the intestine, TAS2Rs act as nutrient sensors that regulate hormone secretion and metabolic signaling pathways. These receptors belong to the G protein-coupled receptor (GPCR) family and trigger a gustducin-mediated signaling cascade that induces intracellular Ca^{2+} release, subsequently activating the transient receptor potential channel TRPM5 and promoting membrane depolarization, which ultimately enhances GLP-1 secretion [8,9]. Among the TAS2R family members, human TAS2R38 (the human ortholog of Tas2r138) has attracted particular attention due to its prominent expression in the gastrointestinal tract and its functional association with incretin hormone secretion [10]. The murine STC-1 enteroendocrine cell line expresses Tas2r138 and its downstream signaling components, providing a robust *in vitro* model for studying intestinal incretin secretion [11,12]. Nevertheless, the potential for natural bitter substances to exert antidiabetic effects through the TAS2R38-mediated gut–hormone pathway has not been systematically investigated.

Trigonella foenum-graecum L. (Fabaceae), commonly known as fenugreek, is a traditional medicinal herb characterized by its distinct bitter taste and warm nature according to the Chinese Pharmacopoeia. Modern pharmacological studies have demonstrated that extracts and bioactive compounds derived from fenugreek exert multiple beneficial metabolic effects, including improving IR and reducing blood glucose levels [13,14]. Several constituents of fenugreek, such as trigonelline, flavonoids, and saponins, have been reported to protect pancreatic islets and enhance GLP-1 secretion [15–17]. However, whether the characteristic "bitterness" of fenugreek serves as a direct pharmacological signal to activate intestinal bitter taste signaling and subsequently modulate the gut-pancreas axis remains a significant scientific question.

In the present study, we aimed to identify the bioactive components of fenugreek extract (FGE) and systematically elucidate its pharmacological mechanisms in T2DM. Using a combination of diabetic mouse models and STC-1 cells, we investigated whether FGE regulates glucose metabolism through the activation of intestinal bitter taste receptor signaling. By integrating pharmacological experiments, ultra-performance liquid chromatography tandem mass spectrometry (UPLC-MS/MS) chemical profiling, and computational simulations, we explored the intestinal Tas2r138-GLP-1-pancreatic insulin signaling axis underlying the therapeutic effects of FGE. We hypothesized that FGE improves glucose metabolism by activating intestinal bitter taste signaling, thereby stimulating endogenous GLP-1 secretion and enhancing pancreatic insulin release to restore metabolic homeostasis.

2. Materials and Methods

2.1. Materials and Reagents

The dried mature seeds of *Trigonella foenum-graecum* L. (Fabaceae) were obtained from Qinghai Province, China. The accepted botanical name has been verified and updated using the Plants of the World Online (POWO) database (http://www.plantsoftheworldonline.org). The botanical materials were formally authenticated by Professor Chunlin Long, an expert in ethnobotany and plant taxonomy at Minzu University of China. Trigonelline (CAS: 535-83-1, purity ≥ 98%) was purchased from Beijing Solarbio Science & Technology Co., Ltd. (Beijing, China). Antibodies against PI3K (12721), phospho-GSK-3β (9336), and GSK3β (8047S) were obtained from Cell Signaling Technology (Danvers, MA, USA). Anti-AKT (ab80588) and anti-phospho-AKT (ab1068) antibodies were purchased from Abcam (Cambridge, UK). Antibodies against TAS2R38 (DF10267, although commercially designated against the human target, this antibody possesses manufacturer-validated specific cross-reactivity with the murine ortholog TAS2R138) and PLCβ2 (DF4721) were obtained from Affinity Biosciences (Changzhou, China). Antibodies against GNAT3 (A15982), β-actin (AC026), and HRP-conjugated goat anti-rabbit IgG (AS014) were obtained from ABclonal Technology (Wuhan, China). All other reagents were of analytical grade unless otherwise specified. The murine enteroendocrine cell line STC-1 was purchased from the Beijing Beina Chuanglian Biotechnology Research Institute (Beijing, China) (Product No. BNCC342403; Batch No. 220715).

2.2. Preparation of Fenugreek Extract (FGE)

Fenugreek seeds were pulverized into a fine powder and extracted using a standardized aqueous decoction method. Briefly, the powdered material was refluxed with 10 volumes of distilled water (at a solid-to-liquid ratio of 1:10, *w*/*v*) for 1 h. The extraction was repeated twice, followed by filtration and concentration under reduced pressure. The concentrated extract was subsequently lyophilized to obtain a stable dry powder, yielding approximately 20% (*w*/*w*, corresponding to a native drug-to-extract ratio of 5:1). The FGE powder was stored at −20 °C and reconstituted in distilled water immediately prior to oral administration. A single standardized batch of lyophilized FGE was used throughout the entire study to eliminate batch-to-batch variability.

2.3. Animal Experiments and T2DM Induction

Specific pathogen-free (SPF) male C57BL/6J mice (7 weeks old, 22.0 ± 0.8 g) were purchased from SiPeiFu Biotechnology Co., Ltd. (Beijing, China; SCXK (Beijing) 2019-0010). Male mice were exclusively selected to eliminate the confounding effects of the female estrous cycle and estrogen fluctuations on insulin sensitivity and lipid metabolism. The sample size (n = 10 per group) was determined a priori via a power analysis for detecting biologically significant differences in fasting blood glucose, factoring in potential

long-term attrition. The study was reported in accordance with the ARRIVE guidelines. Animals were housed under controlled conditions (temperature 23 ± 2 °C, humidity 50–60%, 12-h light/dark cycle) with ad libitum access to food and water. The animal experimental ethics for this study were approved by the Biological and Medical Ethics Review Committee of Minzu University of China (approval number: ECMUC2023005CAAA; Approval Date: 19 September 2023), and all procedures complied with the Guide for the Care and Use of Laboratory Animals.

After one week of acclimatization, mice were randomly assigned to a control group or a T2DM model group using a computer-generated randomization sequence. The T2DM model group was fed a high-fat diet (HFD, 60% of total calories from fat, D12492) for 12 weeks, while the control group received a normal diet (10% of total calories from fat, D12450B). This prolonged HFD feeding induces severe systemic insulin resistance, which partially protects the pancreatic β-cells from subsequent complete STZ-mediated ablation. Following the HFD period, T2DM was induced in the T2DM model group via intraperitoneal injections of streptozotocin (STZ, 50 mg/kg) for three consecutive days [18]. This combination of prolonged HFD feeding and multiple low-dose STZ injections accurately recapitulates the metabolic hallmarks of human T2DM, distinguishing it from T1DM models induced by a single high dose of STZ that results in absolute insulin deficiency. Following the final STZ injection, mice exhibiting a fasting blood glucose (FBG) ≥ 11.1 mmol/L (after a 10-h fast) were considered successfully modeled and included in the study; the successful induction rate was approximately 90%. Mice failing to meet this criterion were excluded prior to randomization. Notably, the mortality rate during the induction and the 4-week treatment phase was 0%. Control mice received an equal volume of citrate buffer. Upon successful establishment of T2DM, mice were randomly assigned to four groups ($n = 10$ per group): T2DM model, metformin (0.25 g/kg), FGE high-dose (FGE-H, 0.52 g/kg), and FGE low-dose (FGE-L, 0.26 g/kg). Treatments were administered via oral gavage once daily for four weeks, while the control and T2DM model groups received distilled water. At the end of the experiment, mice were deeply anesthetized by intraperitoneal injection of tribromoethanol (250 mg/kg; Nanjing Aibei Biotechnology Co., Ltd., Nanjing, China), and peripheral blood was collected from the posterior orbit. Subsequently, manual cervical dislocation was immediately performed to confirm death, followed by tissue collection. Histological and biochemical outcome assessments were performed by independent investigators blinded to the group allocations.

2.4. STC-1 Cell Culture and Pharmacological Interventions

STC-1 enteroendocrine cells were cultured in Dulbecco's Modified Eagle Medium (DMEM, high glucose; Gibco, Thermo Fisher Scientific, Grand Island, NY, USA) supplemented with 10% (v/v) heat-inactivated fetal bovine serum (FBS; Gibco, Thermo Fisher Scientific, Grand Island, NY, USA), 100 U/mL penicillin(Procell, Wuhan Pricella Biotechnology Co., Ltd., Wuhan, China), and 100 µg/mL streptomycin (Gibco, Thermo Fisher Scientific, Grand Island, NY, USA) under standard conditions (37 °C, 5% CO_2). Cells were seeded at a density of 1×10^5 cells/well. A preliminary CCK-8 assay confirmed that trigonelline up to 0.2 mM exhibited no cytotoxicity. Trigonelline was dissolved directly in complete culture medium, while all inhibitors were dissolved in DMSO (final vehicle concentration < 0.1%). To evaluate dose-dependent effects, cells were exposed to trigonelline at concentrations of 0.05 mM, 0.1 mM, and 0.2 mM. For the inhibitor experiments, cells were assigned to four groups: control, trigonelline (TR, 0.2 mM), trigonelline plus Gallein (Gβγ inhibitor, 10 µM), and trigonelline plus U73122 (PLC inhibitor, 10 µM) Inhibitor groups were pre-incubated with their respective agents for 30 min prior to a 2-h trigonelline treatment for GLP-1 secretion assays. All in vitro experiments were performed with four independent biological

replicates ($n = 4$). Intracellular Ca^{2+} levels were measured using a Fluo-4 calcium assay kit, and GLP-1 secretion was quantified using a commercial enzyme-linked immunosorbent assay (ELISA) kit according to the protocols.

2.5. OGTT and Metabolic Parameter Assessment

After four weeks of treatment, blood samples were collected from the posterior orbit following a 10-h fast. The blood glucose levels were measured using a glucometer. The triglyceride (TG), total cholesterol (TC), as well as liver and kidney function indicators were measured with the corresponding kits. An OGTT was performed by orally administering glucose (2 g/kg), with blood glucose monitored at 0, 30, 60, 90, and 120 min. The AUC was calculated to evaluate glucose tolerance. Serum insulin and GLP-1 levels were determined using commercial ELISA kits. A DPP-4 inhibitor (10 μL/mL blood) was added immediately to the collection tubes to prevent incretin degradation, and total GLP-1 levels were quantified. Ileal tissue GLP-1 concentrations were normalized to total tissue protein content. The Homeostatic Model Assessment for Insulin Resistance (HOMA-IR) was calculated as: [Fasting Insulin (μU/mL) × FBG (mmol/L)]/22.5. The TyG index was calculated as: Ln [Fasting TG (mg/dL) × FBG (mg/dL)/2].

2.6. Histopathological and Immunofluorescence Evaluation

The ileal, pancreatic tissues, liver, and kidney were fixed, embedded in paraffin, and sectioned for examination. HE staining was performed on all tissues, alongside Periodic acid-Schiff (PAS) staining specifically for renal sections, to evaluate morphological alterations. Images were captured via light microscopy. Importantly, all digital image acquisitions and subsequent semi-quantitative morphological analyses (e.g., lipid droplet area percentage, glomerulosclerosis score, villus length, islet area, and fluorescence intensity) using Fiji (ImageJ, version 1.54f) were performed by an independent investigator who was strictly blinded to the experimental group allocations. To detail the exact scoring methods, hepatic lipid accumulation was quantified by measuring the percentage of the lipid droplet area relative to the total tissue area using the thresholding function in ImageJ. Renal glomerulosclerosis was evaluated semi-quantitatively on a scale of 0 to 4 based on the degree of mesangial matrix expansion and capillary obliteration (0 = normal; 1 = <25%; 2 = 25–50%; 3 = 50–75%; 4 = >75% of the glomerular cross-sectional area). Additional morphometric parameters included villus length and islet area. For immunofluorescence, pancreatic sections were incubated with primary antibodies against GLP-1 and GLP-1R, followed by fluorescently labeled secondary antibodies. Fluorescence intensity was quantified using ImageJ software to assess protein expression and localization.

2.7. Gene and Protein Expression Analysis

Total RNA was extracted and reverse-transcribed into cDNA using standard protocols. Relative mRNA expression levels were quantified via RT-qPCR using the $2^{-\Delta\Delta CT}$ method, with Gapdh as the internal control. Primer sequences are provided in Tables S1 and S2. For protein analysis, tissues were homogenized in RIPA lysis buffer containing protease and phosphatase inhibitors. Equal amounts of protein, determined by BCA assay, were separated by SDS-PAGE and transferred onto PVDF membranes. Membranes were incubated overnight at 4 °C with primary antibodies against PI3K, AKT, p-AKT, GSK3β, p-GSK3β, TAS2R38 (utilized to detect the murine TAS2R138 protein), GNAT3, PLCβ2, and β-actin. Following incubation with HRP-conjugated secondary antibodies, protein bands were visualized via ECL and quantified using ImageJ. All Western blot and RT-qPCR analyses were performed with at least three independent biological replicates ($n = 3$). Target protein band intensities were normalized to the endogenous control (β-actin); however, phosphorylated

proteins (e.g., p-AKT, p-GSK3β) were appropriately normalized to their respective total protein levels.

2.8. Chemical Profiling via UPLC-MS/MS and Absolute HPLC Quantification

To identify FGE-derived constituents in the ileum, mice were administered FGE (0.52 g/kg) for seven consecutive days. Based on preliminary gastrointestinal transit experiments, ileal tissues were collected 15 min after the final oral dose. To definitively exclude unabsorbed luminal contamination, the excised ileal segments were longitudinally opened and rigorously flushed with ice-cold PBS three times until the effluent was completely clear prior to homogenization. UPLC-MS/MS analysis was performed on the FGE and ileal tissue samples from both T2DM model and FGE-treated mice under positive and negative ion modes. The untargeted metabolomic profiling was conducted using a Thermo UHPLC vanquish system coupled with a QExactive HF-X mass spectrometer (Thermo Fisher Scientific, Bremen, Germany). Chromatographic separation was achieved on an ACQUITY UPLC HSS T3 column (2.1 mm × 100 mm, 1.8 μm; Waters Corporation, Milford, MA, USA) maintained at 35 °C, with a flow rate of 0.3 mL/min. The mobile phase consisted of 0.1% formic acid in water (A) and 0.1% formic acid in acetonitrile (B). Mass spectrometry data (scan range 90–1300 m/z) were processed using XCMS software for peak alignment and extraction. Compound identification was established by matching against standard spectral databases, utilizing strict criteria of an MS1 mass error < 15 ppm and an MS2 fragment similarity score > 0.7.

Furthermore, the absolute content of the principal bioactive marker, trigonelline, in the lyophilized FGE powder was quantitatively determined using an HPLC system equipped with a Variable Wavelength Detector (VWD). The detection wavelength was set at 265 nm, and the injection volume was 5.0 μL. Absolute quantification was performed using a high-purity authentic reference standard. The method was thoroughly validated for precision (RSD $< 3\%$), recovery (98.5–101.2%), Limit of Detection (LOD = 0.15 μg/mL), and Limit of Quantification (LOQ = 0.48 μg/mL). A single standardized batch of lyophilized FGE powder was used throughout the entire study to ensure extract consistency and eliminate batch-to-batch variability.

2.9. Network Pharmacological Analysis

A comprehensive search was performed using the TCMSP, SwissTargetPrediction, and PharmMapper databases based on the identified chemical constituents of FGE. The GSE25724 dataset (comprising human pancreatic islet transcriptomes from 6 T2DM patients and 7 non-diabetic controls) was utilized to obtain differentially expressed genes (DEGs) from T2DM samples. The raw microarray expression data were log2-transformed and normalized using the Robust Multi-array Average (RMA) procedure. DEGs were subsequently identified using the limma package in R, applying a strict threshold of $|\log2FC| > 1$ and a Benjamini–Hochberg adjusted p-value (FDR) < 0.05. Common targets between FGE and T2DM were identified and visualized using a Venn diagram. Gene Ontology (GO) enrichment analysis and Kyoto Encyclopedia of Genes and Genomes (KEGG) pathway enrichment analysis were conducted using R software (version 4.4.0). The enrichment parameters were defined with a significance threshold of adjusted p-value < 0.05, utilizing *Homo sapiens* as the background genome.

2.10. Computational Simulations

For structural analysis, the 3D structure of human TAS2R38 was predicted using AlphaFold2 (evaluating pLDDT confidence scores > 80 for transmembrane domains) and evaluated via the PROCHECK program. Membrane protein systems were constructed

using CHARMM-GUI. Molecular docking between human TAS2R38 and ileal compounds was performed using Autodock Vina, with receptor and ligand preparation conducted using AutoDockTools (version 1.5.7). The grid box was centered at coordinates x = 61.543, y = 74.631, and z = 65.225 to encompass the putative binding pocket. Phenylthiocarbamide (PTC), a well-established TAS2R38 agonist, was utilized as a positive validation control for the docking protocol. To further elucidate the binding stability, molecular dynamics (MD) simulations via GROMACS 2025.2 for 100 ns were conducted. For MD simulations, the receptor was embedded in a POPC lipid bilayer (via CHARMM-GUI). Simulations were performed using the CHARMM36m force field and TIP3P water model (neutralized with 150 mM NaCl) at 310 K. The system was equilibrated through standard NVT and NPT ensembles prior to the 100 ns production run.

2.11. Statistical Analysis

Statistical evaluations were performed using GraphPad Prism 8.0.1. In this study, data are expressed as mean ± standard deviation (SD). Data normality and variance homogeneity were verified using the Shapiro–Wilk and Levene's tests, respectively. Comparisons among multiple groups at a single time point were analyzed using one-way analysis of variance (ANOVA) followed by Tukey's post hoc test. Longitudinal repeated measurements (e.g., dynamic body weight, dietary energy intake, and OGTT) were analyzed via two-way repeated-measures ANOVA (RM-ANOVA) followed by Bonferroni's post hoc test. A p value < 0.05 was considered statistically significant.

3. Results

3.1. FGE Ameliorates Systemic Metabolic Dysregulation in T2DM Mice

As outlined in the experimental schematic (Figure 1A), T2DM was successfully induced in mice. A classic clinical manifestation of diabetes is hyperphagia (excessive eating) accompanied by body weight loss. During the 4-week treatment phase, dynamic metabolic monitoring revealed that the T2DM model mice exhibited significantly elevated daily energy intake (kcal/day/mouse) and progressive body weight loss compared to the normal chow-fed control group. Notably, both FGE and metformin administration effectively suppressed this hyperphagia, restoring energy consumption to near-normal levels while maintaining stable body weight trajectories (Figure 1B). Furthermore, the T2DM model exhibited significantly elevated fasting (FBG) and random blood glucose (RBG) levels, along with compensatory hyperinsulinemia (elevated insulin levels), confirming severe metabolic impairment. FGE administration, as well as the positive control metformin (0.25 g/kg), markedly reduced both FBG and RBG levels, and successfully alleviated the hyperinsulinemia (Figure 1C).

OGTT results further demonstrated that glucose tolerance was severely impaired in T2DM model mice. Conversely, both FGE and metformin treatments not only improved glucose clearance, as evidenced by decreased AUC values, but also significantly mitigated systemic insulin resistance, as reflected by a reduced HOMA-IR index (Figure 1D). Beyond glycemic control, lipid metabolism was significantly dysregulated in T2DM mice; systemic TG and TC levels were markedly elevated in the T2DM model group but were significantly attenuated following either FGE or metformin treatment. Consistently, the TyG index was significantly decreased in the treatment groups (Figure 1E). These findings indicate that FGE effectively mitigates hyperphagia, restores glucose tolerance, and ameliorates lipid metabolic disorders in T2DM.

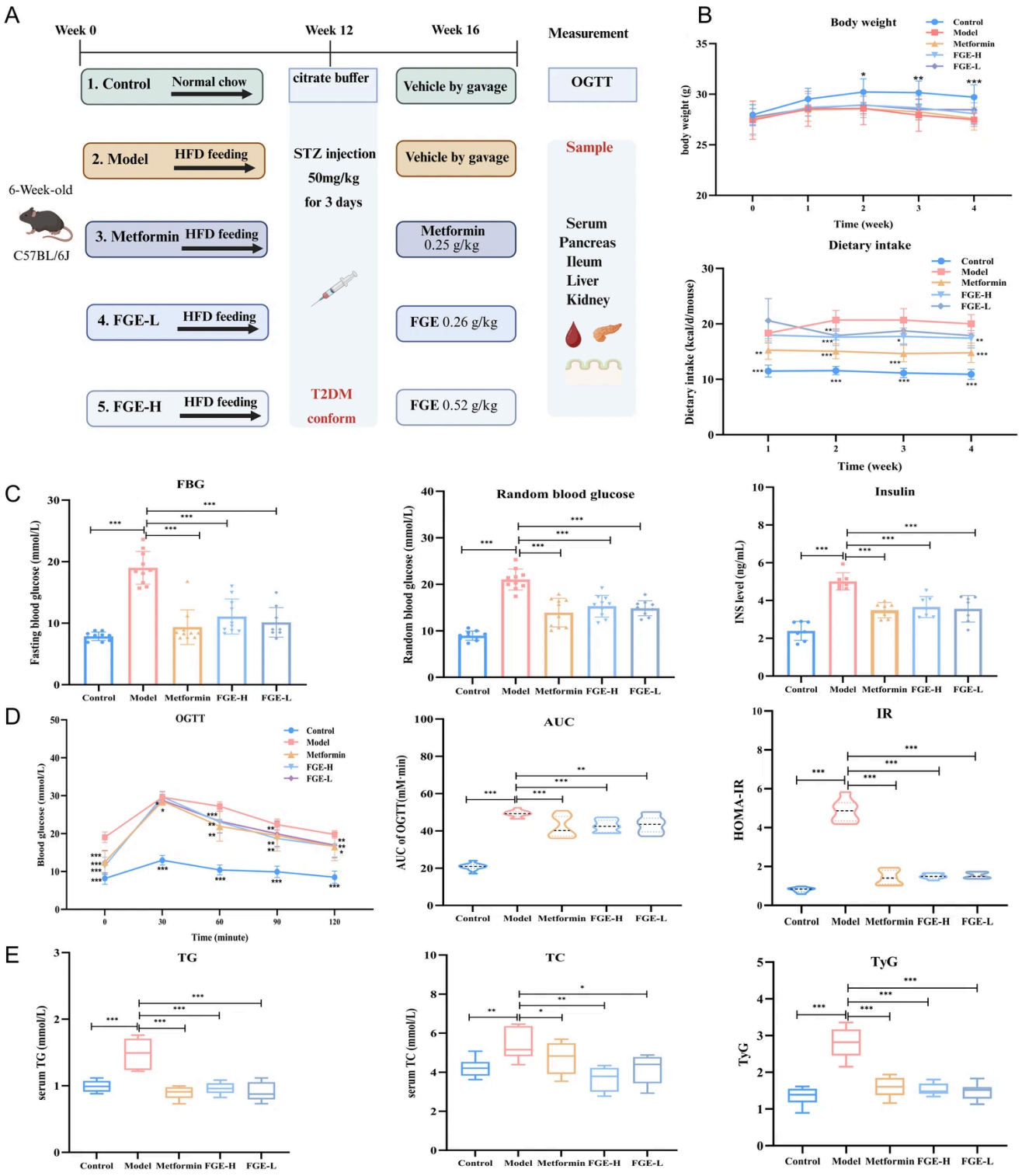


Figure 1. FGE Ameliorates Systemic Metabolic Dysregulation in T2DM Mice. (**A**) Schematic representation of the in vivo experimental design. (**B**) Dynamic monitoring of body weight and daily dietary intake during the 4-week treatment period. (**C**) Fasting blood glucose (FBG), random blood glucose (RBG), and serum insulin levels measured after four weeks of treatment. (**D**) Blood glucose excursion curve during the oral glucose tolerance test (OGTT), area under the curve (AUC) analysis, and Homeostatic Model Assessment of Insulin Resistance (HOMA-IR). (**E**) Serum levels of triglycerides (TG), total cholesterol (TC), and triglyceride–glucose (TyG) index. Data are expressed as mean ± SD ($n = 10$). Statistical significance is indicated as follows: $p < 0.05$ (*), $p < 0.01$ (**), and $p < 0.001$ (***).

Furthermore, the in vivo safety profile of FGE was systematically evaluated. Histopathological examinations revealed that both FGE and metformin treatments alleviated hepatic lipid droplet accumulation (indicated by a significantly reduced lipid droplet percentage area, Figure S1A). Renal histological analysis demonstrated that FGE and metformin treatment improved glomerular morphological alterations, as evidenced by the restoration of glomerular cross-sectional area in H&E-stained sections (Figure S1B). In addition, PAS staining and semi-quantitative analysis showed that both treatments significantly reduced glomerulosclerosis scores compared with the T2DM model group (Figure S1C). Consistently, treatments did not adversely affect liver (Figure S1D) or kidney indices (Figure S1E) and maintained the serum levels of ALT, AST, BUN, and CRE within stable physiological ranges, indicating that FGE displayed an acceptable safety profile without evident macroscopic organ toxicity at the tested doses.

3.2. FGE Potentiates GLP-1 Secretion and Restores Tissue Morphology

To uncover the endocrine mechanisms driving the systemic metabolic improvements observed in FGE-treated mice, we investigated the GLP-1-mediated inter-organ crosstalk. Given the central role of GLP-1 in metabolic regulation, its levels in serum and ileal tissues were quantified. GLP-1 concentrations were significantly lower in the T2DM model group than in the control group, while both FGE and metformin administration triggered a robust increase in GLP-1 levels in both systemic circulation and ileal tissues (Figure 2A). Immunofluorescence analysis confirmed that the expression of GLP-1 and GLP-1R within pancreatic tissues was significantly upregulated after FGE and metformin treatments compared with the T2DM model group (Figure 2B). FGE and metformin treatments significantly preserved intestinal integrity, as indicated by restored villus architecture and quantitatively increased villus length (Figure 2C). Pancreatic histology further showed that islet structures in T2DM mice were disrupted and diminished in size. In contrast, FGE and metformin treatments markedly improved overall islet morphology and significantly increased the islet area (Figure 2D).

3.3. FGE Enhances Pancreatic Insulin Signaling via the Canonical GLP-1R/PI3K-AKT Axis

To systematically elucidate how the FGE-induced elevation of GLP-1 restores pancreatic function, we focused on the downstream intracellular signaling within pancreatic islets. A network pharmacology analysis was initially performed. The intersection of putative FGE targets and T2DM-related genes identified multiple potential therapeutic targets (Figure 3A,B). Subsequent GO and KEGG pathway enrichment analyses revealed that these targets were significantly enriched in multiple core pathways, with the PI3K-AKT signaling cascade emerging as a prominent candidate (Figure 3C,D). Given the well-established physiological paradigm that circulating GLP-1 binds to the pancreatic GLP-1R to promote β-cell survival and glucose-dependent insulin secretion predominantly via the PI3K-AKT-GSK3β signaling cascade, we further evaluated the downstream intracellular mechanisms within the pancreatic tissue to confirm the functionality of this inter-organ communication. RT-qPCR analysis confirmed that insulin secretion and cell survival-associated genes, including *Pdx1*, *Irs1*, *Irs2*, *Insr*, and *Ins*, were significantly downregulated in T2DM mice but were robustly upregulated after both FGE and metformin treatments (Figure 3E). Consistent with these transcriptional changes, Western blot analysis demonstrated that FGE and metformin significantly increased the protein levels of PI3K and the ratio of phosphorylated AKT to total AKT (p-AKT/Total AKT), while concurrently suppressing the expression of GSK3β (Figure 3F). These findings strongly indicate that the FGE-induced elevation of systemic GLP-1 functionally engages the pancreatic GLP-1R to orchestrate downstream insulin signaling and β-cell preservation.

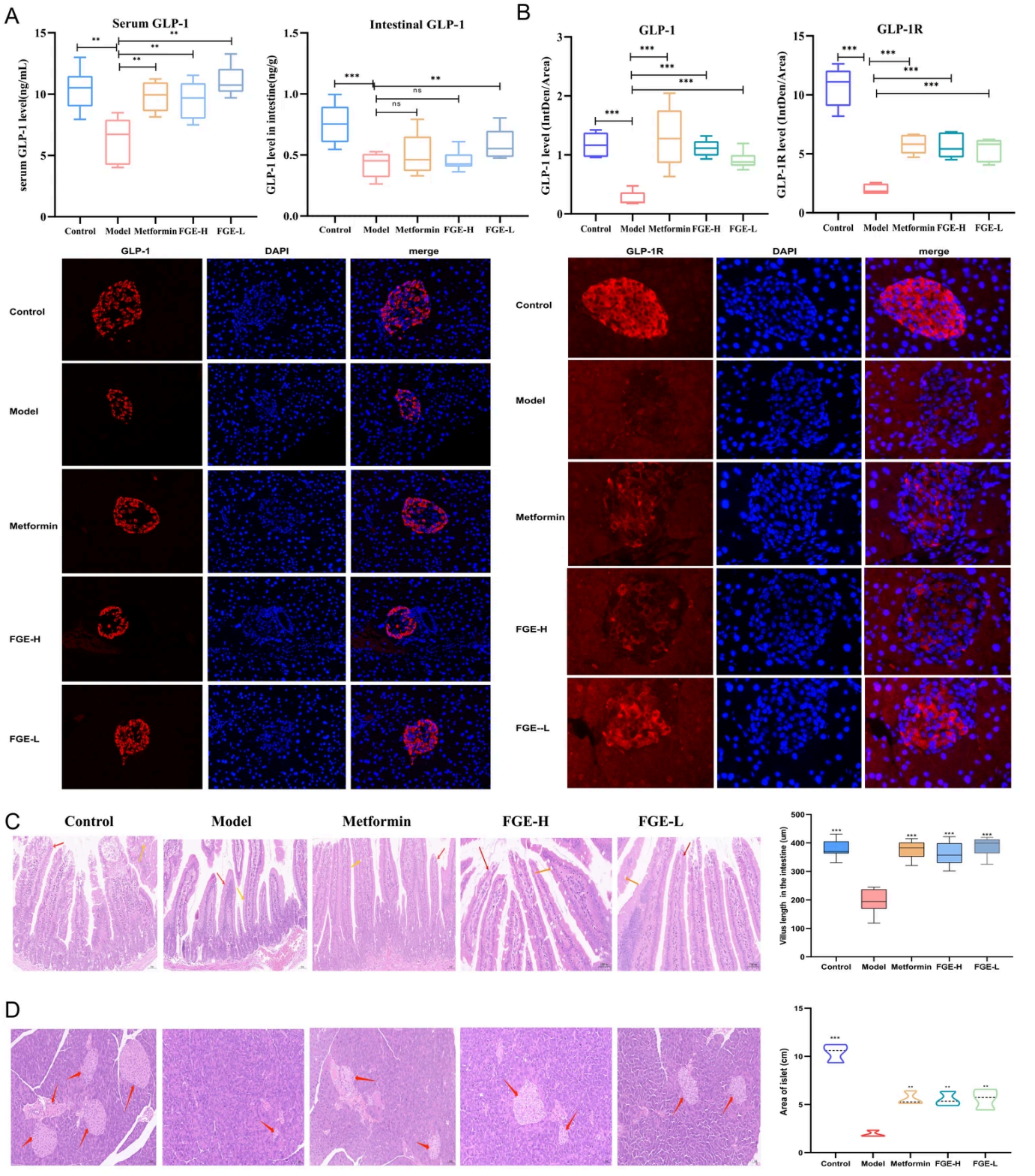


Figure 2. FGE potentiates GLP-1 secretion and restores intestinal and pancreatic morphology. (**A**) GLP-1 concentrations in serum and ileal tissues quantified by ELISA. (**B**) Immunofluorescence analysis of GLP-1 and GLP-1R expression in pancreatic islets. (**C**) Representative HE staining images of ileal tissues and quantitative analysis of villus length. The red arrows indicate small intestinal villi, while the yellow arrows indicate goblet cells. (**D**) Representative HE staining images of pancreatic tissues and quantitative analysis of islet area. The red arrows indicate pancreatic β-cells. Data are expressed as mean ± SD ($n = 10$). Statistical significance compared with the model group is indicated as follows: $p < 0.01$ (**), and $p < 0.001$ (***).

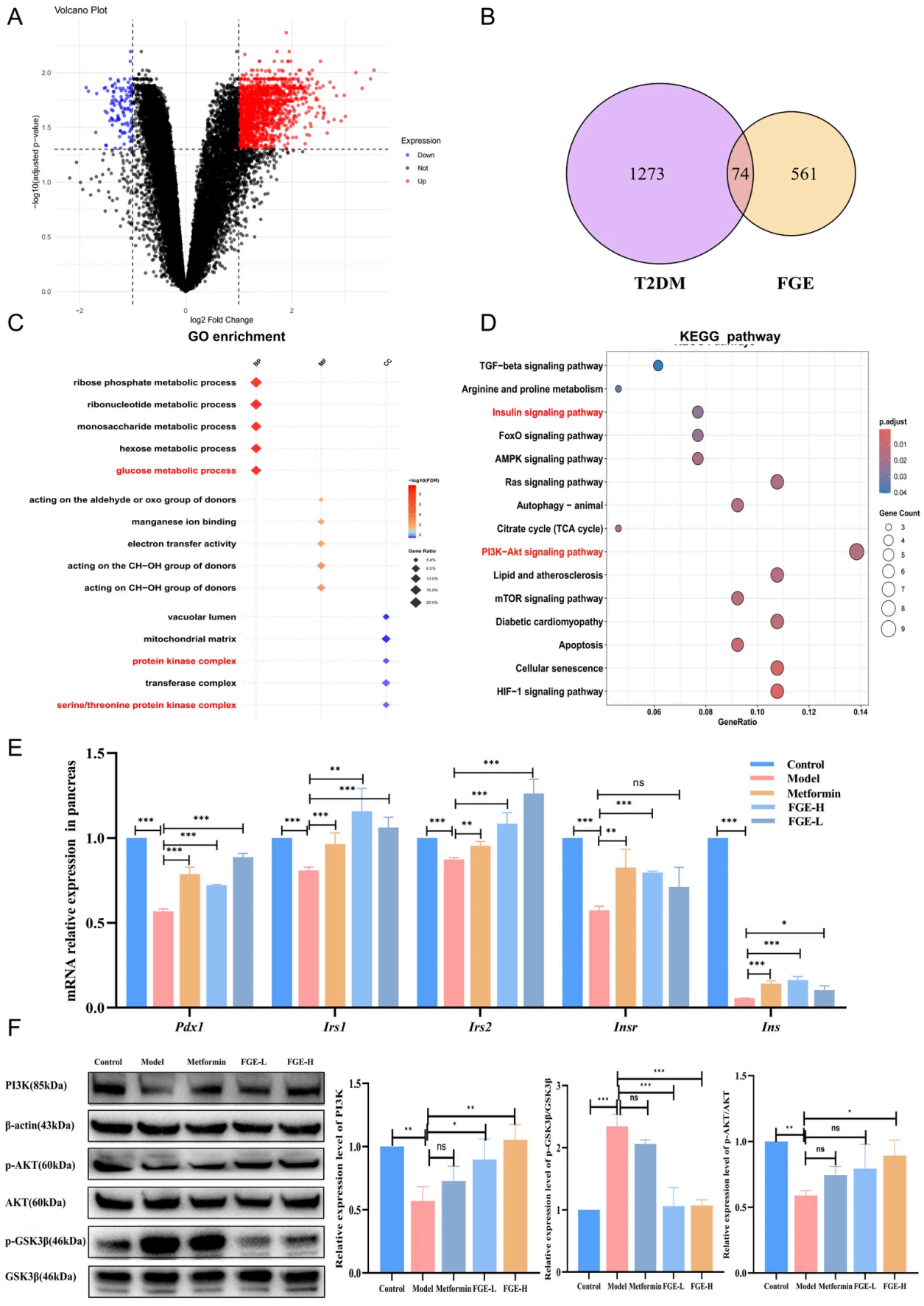


Figure 3. FGE enhances pancreatic insulin signaling via the canonical GLP-1R/PI3K-AKT axis. (**A**) Volcano plot illustrating the differentially expressed genes (DEGs) associated with T2DM pathogenesis.

(**B**) Venn diagram demonstrating the intersection of putative targets of FGE-derived constituents and T2DM-associated genes. (**C**) Gene Ontology (GO) functional enrichment analysis of the overlapping targets. (**D**) Kyoto Encyclopedia of Genes and Genomes (KEGG) pathway enrichment analysis, highlighting the top significantly enriched signaling pathways modulated by FGE intervention. The pathway map was reproduced with permission from the KEGG database. (**E**) Relative mRNA expression of insulin secretion-related genes (*Pdx1*, *Irs1*, *Irs2*, *Insr*, and *Ins*) in pancreatic tissues. (**F**) Representative Western blot images and quantitative analysis of PI3K, phosphorylated AKT (p-AKT), total AKT, phosphorylated GSK3β (p-GSK3β), and total GSK3β protein expression in the pancreas. Data are expressed as mean ± SD ($n = 3$). Statistical significance compared with the model group is indicated as follows: $p < 0.05$ (*), $p < 0.01$ (**), and $p < 0.001$ (***).

3.4. FGE Activates the Intestinal Tas2r138-Mediated Bitter Taste Signaling Cascade

Having established that FGE restores metabolism via the GLP-1/pancreas axis, we next sought to identify the upstream gastrointestinal sensor responsible for triggering this endogenous GLP-1 release. To determine whether FGE regulates GLP-1 secretion via intestinal bitter taste receptors, the spatial expression of *Tas2r138* was examined. Under physiological conditions, *Tas2r138* mRNA expression was most prominent in the colon and ileum. While T2DM induced a significant downregulation of *Tas2r138*, FGE treatment effectively restored its expression, particularly in the ileum (Figure 4A). Further RT-qPCR analysis revealed that genes encoding the bitter taste signaling machinery, including *Tas2r138*, *Gnat3*, *Plcb2*, *Itpr3*, and *Trpm5*, were significantly downregulated in the T2DM model group but markedly upregulated following FGE treatment (Figure 4B). Consistently, Western blot analysis demonstrated that the protein levels of TAS2R138, GNAT3, and PLCβ2 were significantly increased following FGE administration (Figure 4C,D). Notably, while the positive control metformin effectively improved downstream systemic metabolic parameters, it failed to significantly upregulate the expression of intestinal bitter taste signaling components compared to the T2DM model group. This crucial distinction highlights that while metformin operates primarily through classical systemic metabolic pathways, FGE specifically targets and activates the TAS2R38-mediated bitter taste cascade within the gut mucosa to exert its unique therapeutic effects.

3.5. Bioactive Identification and Mechanistic Validation of Trigonelline

To conclusively link the complex FGE to the activation of the intestinal bitter taste receptor, we performed chemical profiling and in vitro mechanistic validations. UPLC-MS/MS analysis identified multiple FGE-derived constituents in ileal tissues, including trigonelline, orientin, isoorientin, isovitexin, and dioscin (Figure 5A,B and Table S3). Crucially, absolute quantitative HPLC analysis revealed that the content of trigonelline in the lyophilized FGE powder was 15.1 mg/g, calculated based on a five-point standard curve ($R^2 = 0.9992$). The corresponding standard calibration curve and chromatograms are presented in Figure S2A,B. Evaluation of the predicted structure of the TAS2R38 receptor and its bilayer conformation was displayed in Figure S3A,B. Molecular docking revealed that these compounds, including trigonelline, exhibited favorable predicted docking interactions toward the TAS2R38 receptor, with docking scores lower than −6.0 kcal/mol (Figure 5C). To validate the reliability of our defined docking pocket, we evaluated Phenylthiocarbamide (PTC), a classic known TAS2R38 agonist, which yielded a strong benchmark docking score of −6.2 kcal/mol. The docking score of trigonelline was comparable to this known active ligand, underscoring its structural viability as a putative natural ligand. Detailed three-dimensional (3D) binding poses, specific interaction sites, and hydrogen-bonding distances between these identified FGE-derived compounds and the TAS2R38 receptor are comprehensively illustrated in Figure S3C. Although several constituents exhibited

comparable docking profiles, trigonelline was strategically selected as the representative ligand for downstream in vitro validation. This selection was driven by its status as the official pharmacopoeial quality-control marker of fenugreek, its high local mucosal exposure confirmed by our ileal UPLC-MS/MS profiling, and its intrinsic chemical nature as a potent bitter alkaloid, which perfectly aligns with the physiological function of the bitter taste sensor. The results of MD simulations between TAS2R38 and trigonelline suggested that they form a stable complex (Figure 5D). To validate these findings, STC-1 cells were treated with trigonelline, which significantly stimulated GLP-1 secretion and increased intracellular Ca^{2+} flux (Figure 5E,F). Furthermore, trigonelline upregulated the transcription of *Tas2r138*, *Gnat3*, *Plcb2*, *Itpr3*, and *Trpm5* (Figure 5G). Notably, the trigonelline-induced hormone secretion and signaling activation were significantly blunted by the PLC inhibitor U73122 or the Gβγ inhibitor Gallein (Figure 5H–J). These findings mechanistically confirm that trigonelline promotes GLP-1 secretion through a Gβγ/PLC-dependent pathway, which is consistent with Gq-coupled receptor activation.

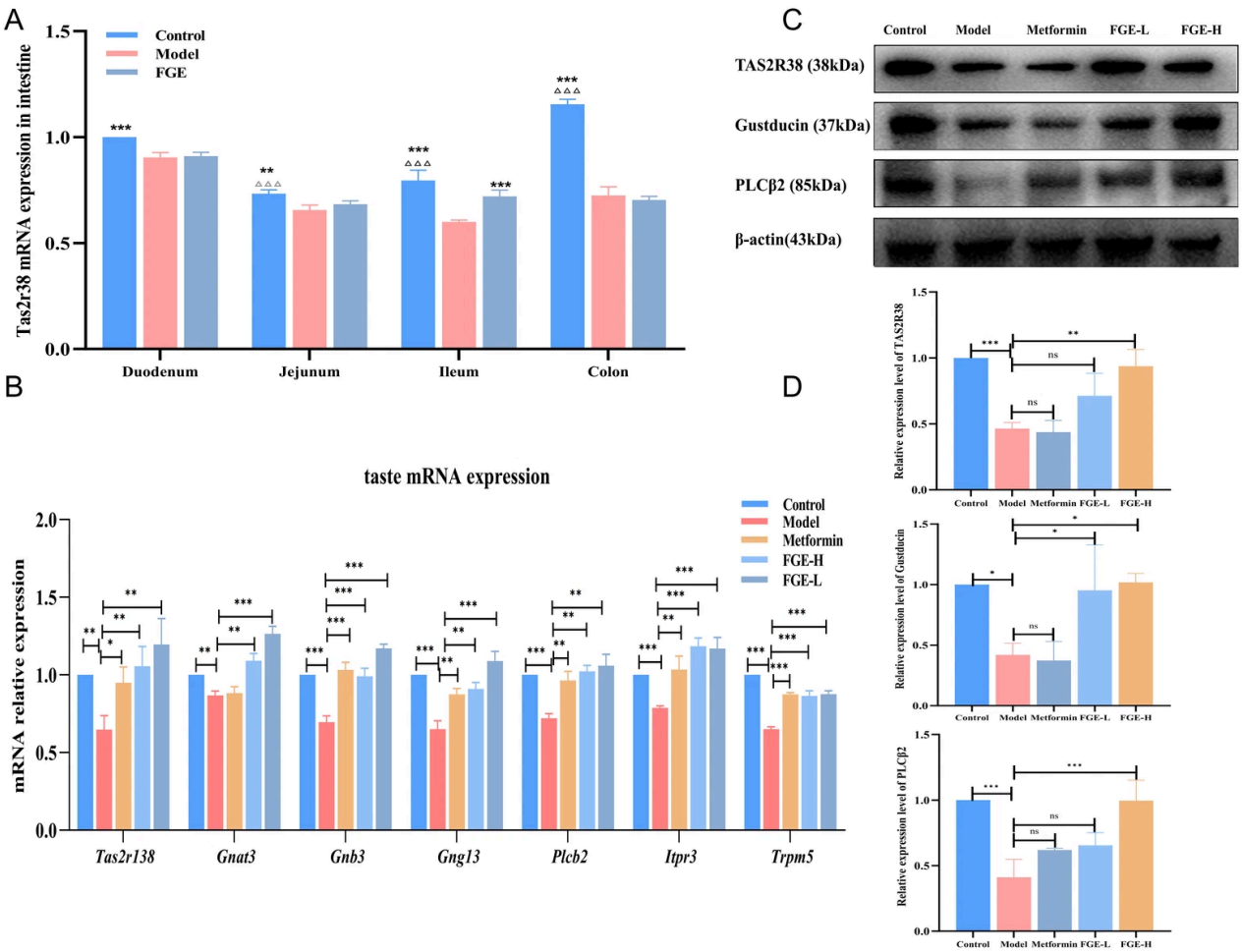


Figure 4. FGE activates the intestinal TAS2R38-mediated bitter taste signaling cascade. (**A**) Relative mRNA expression of *Tas2r138* across different intestinal segments (duodenum, jejunum, ileum, and colon) determined by RT-qPCR. The dosage of FGE administered was 0.52 g/kg. Expression levels were normalized to GAPDH, with the duodenal Control group set to 1. $p < 0.05$ (*), $p < 0.01$ (**), and $p < 0.001$ (***) vs. the corresponding Model group; $p < 0.001$ (△△△) vs. the duodenal Control group. (**B**) RT-qPCR analysis of bitter taste signaling-related genes (*Tas2r138*, *Gnat3*, *Plcb2*, *Itpr3*, and *Trpm5*) in ileal tissues. (**C**) Representative Western blot images and (**D**) quantitative densitometric analysis of TAS2R138, GNAT3, and PLCβ2 protein expression in the ileum. β-actin was utilized as the internal loading control. Data are expressed as mean ± SD ($n = 3$).

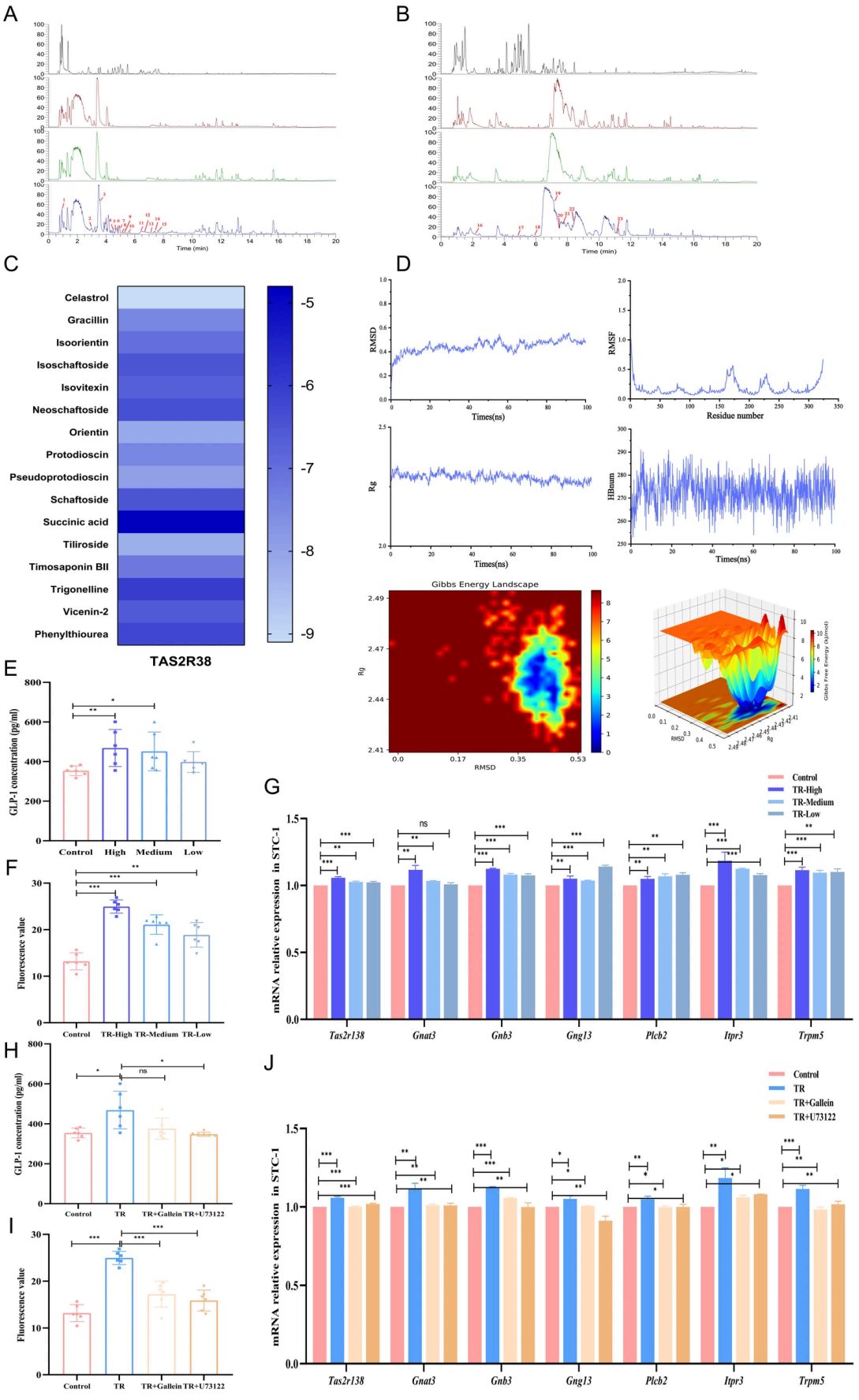


Figure 5. Identification of FGE−derived constituents and mechanistic validation of trigonelline in STC−1 cells. UPLC-MS/MS total ion chromatograms of constituents in ileal tissue of T2DM model

mices after FGE treatment under positive (**A**) and negative ion modes (**B**). From top to bottom, the samples are as follows: FGE, ileum tissue combined with FGE, ileum tissue from the T2DM model group, and ileum tissue from the FGE group. The components of FGE distributed in the ileal tissue are indicated in red. (**C**) Molecular docking poses and predicted docking scores of selected FGE−derived compounds with human TAS2R38. (**D**) Molecular dynamics simulation analyses of the TAS2R38−trigonelline complex. (**E**) GLP−1 secretion and (**F**) relative intracellular Ca^{2+} fluorescence intensity in STC−1 cells treated with varying concentrations of trigonelline. (**G**) RT-qPCR analysis of downstream signaling genes in STC−1 cells. Effects of the PLC inhibitor (U73122) and the Gβγ inhibitor (Gallein) on GLP−1 secretion (**H**), Ca^{2+} fluorescence intensity (**I**), and downstream signaling genes (**J**). Data are expressed as mean ± SD ($n = 4$). Compared with the Model group: $p < 0.05$ (*), $p < 0.01$ (**), and $p < 0.001$ (***).

3.6. Proposed Mechanism of FGE in T2DM Treatment

Collectively, our data elucidate a novel "gut-centric" mechanism by which FGE ameliorates T2DM. As illustrated in the mechanism map (Figure 6), FGE and its bioactive component trigonelline activate a Gβγ/PLC-dependent signaling cascade consistent with the intestinal Tas2r138 receptor, triggering the PLCβ2/TRPM5 signaling pathway to stimulate endogenous GLP-1 release. The elevated circulating GLP-1 subsequently engages the pancreatic GLP-1R, activating the PI3K-AKT-GSK3β axis to enhance insulin secretion and preserve β-cell morphology, ultimately restoring systemic glucose homeostasis.

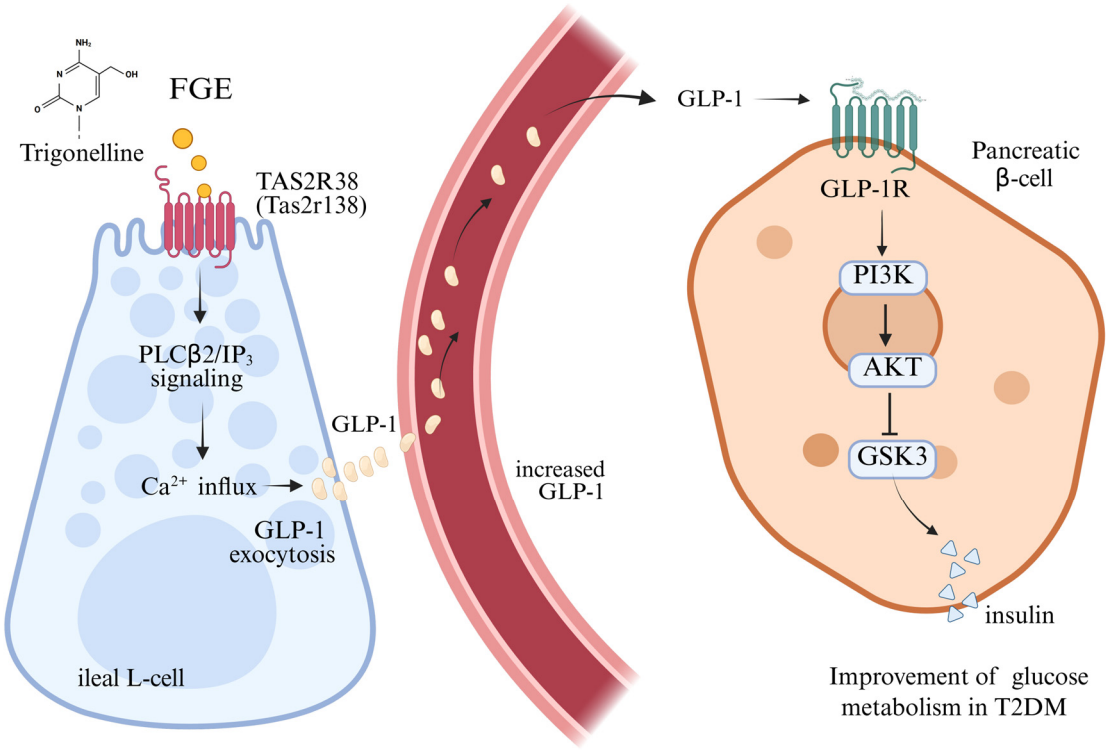


Figure 6. Proposed mechanism of FGE in the treatment of T2DM via the gut-pancreas axis. FGE and the bioactive constituent trigonelline act as a ligand to activate the intestinal TAS2R38 receptor, triggering the PLCβ2/TRPM5 signaling cascade to stimulate the endogenous release of GLP-1 from enteroendocrine L-cells. The elevated circulating GLP-1 subsequently engages the pancreatic GLP-1R, activating the PI3K-AKT-GSK3β signaling pathway. This orchestrated inter-organ communication enhances glucose-dependent insulin secretion, preserves β-cell morphology, and ultimately restores systemic glucolipid homeostasis.

4. Discussion

The combination of a high-fat diet and low-dose STZ is widely used to establish experimental models that faithfully mimic the metabolic hallmarks of T2DM, including IR and pancreatic β-cell dysfunction [19,20]. In the present study, the T2DM model exhibited pronounced disturbances in glucose and lipid metabolism, as evidenced by elevated fasting blood glucose levels and dysregulated lipid profiles. Fenugreek, a traditional herbal medicine with recognized antidiabetic properties, has been previously reported to improve glycemic control [21,22]. Consistent with these findings, our results demonstrated that FGE significantly reduced fasting blood glucose levels and improved glucose tolerance in T2DM mice. In addition to its hypoglycemic effects, FGE exerted beneficial actions on lipid metabolism, significantly decreasing serum TG and TC levels, which aligns with previous reports in hyperlipidemic models [23]. Clinical studies have further supported the efficacy of fenugreek in improving glycemic and lipid profiles in diabetic patients [24]. Taken together, these findings from both animal and clinical studies strongly support the therapeutic potential of FGE in T2DM management.

Based on the body surface area normalization method, the dose of FGE (0.26 g/kg) administered to mice in our study translates to a Human Equivalent Dose of approximately 0.021 g/kg. For a standard 70-kg adult, this equates to roughly 1.48 g of the lyophilized extract per day. Considering the 20% extraction yield, this corresponds to approximately 7.4 g of raw fenugreek seeds. Remarkably, this translated dosage falls perfectly within the standard clinical recommendation stipulated by the Chinese Pharmacopoeia (5–10 g per day). Thus, our chosen experimental dosage not only closely mimics traditional human consumption but also is expected to provide sufficient intestinal mucosal exposure to active bitter alkaloids like trigonelline, serving as a robust proof-of-concept with translational and ethnopharmacological relevance.

Recent emerging evidence has highlighted the physiological functions of taste receptors located in extraoral tissues, particularly the gastrointestinal tract. The activation of intestinal bitter taste receptors has been shown to regulate enteroendocrine hormone secretion, notably GLP-1, which is crucial for glucose homeostasis [25]. In the present study, FGE treatment significantly elevated GLP-1 levels in both serum and ileal tissues, suggesting the intestine serves as a primary target organ for FGE-mediated metabolic regulation. Among the bitter taste receptor family, TAS2R38 is extensively studied and highly expressed in the gastrointestinal tract, where it functionally correlates with both diabetes progression and GLP-1 secretion [10]. A study profiling bitter taste receptors in the digestive tract of C57BL/6 mice indicated abundant *Tas2r138* expression in the colon [26], consistent with our physiological observations [27]. Interestingly, under diabetic conditions, the expression of Tas2r138 was significantly decreased in our model. This downregulation may be consistent with recent pathophysiological findings. Emerging clinical evidence demonstrates that intestinal taste receptors, including TAS2R38, are significantly downregulated in patients with severe obesity and metabolic syndrome, and this decline is negatively correlated with local inflammatory markers such as IL-6 [28]. Consequently, the ileum was selected as the primary site for subsequent mechanistic investigations. Further analyses revealed that FGE significantly upregulated the expression of key genes within the bitter taste signaling cascade, indicating the robust activation of Tas2r138-mediated signaling.

The secretion of GLP-1 from intestinal L-cells is central to mediating communication between the gut and the pancreas, forming the foundational "gut-pancreas axis" that regulates metabolic homeostasis. Upon release into the circulation, GLP-1 binds to the GLP-1R widely expressed on pancreatic β-cells and other organs [29], thereby promoting insulin secretion, cellular proliferation, and β-cell survival [30]. Crucially, beyond its direct pancreatic effects, GLP-1 is a potent anorexigenic hormone that centrally suppresses appetite, delays

gastric emptying, and promotes satiety. Our macroscopic phenotypic data align with this endocrine mechanism: the robust endogenous GLP-1 release triggered by FGE functionally translated into a significant reduction in the severe hyperphagia and stabilization of weight loss observed in T2DM mice. Mechanistically, elevated GLP-1 acts centrally to suppress appetite and delay gastric emptying, leading to reduced caloric intake. Concurrently, by ameliorating systemic insulin resistance and enhancing cellular glucose uptake, FGE halts the severe catabolic tissue breakdown (e.g., muscle and fat wasting) characteristic of uncontrolled diabetes. Thus, the mice eat less but stabilize their body weight because their cellular energy utilization is restored. Consistent with its pancreatic roles, our study demonstrated that FGE treatment significantly improved overall islet morphology and increased the islet area. Furthermore, immunofluorescence analysis revealed that FGE significantly elevated both GLP-1 and GLP-1R expression within pancreatic tissues. While circulating GLP-1 is primarily secreted by the intestine, the observed increase in intra-islet GLP-1 expression may reflect the accumulation of circulating GLP-1 binding tightly to upregulated GLP-1R on β-cells. Additionally, it could result from an intra-islet paracrine adaptation wherein pancreatic α-cells upregulate prohormone convertase 1/3 (PC1/3) under metabolic stress to locally synthesize GLP-1 for β-cell protection [31,32]. Activation of GLP-1R is known to stimulate the downstream PI3K-AKT signaling cascade, a critical pathway for regulating insulin dynamics and cell survival [33]. In the present study, Western blot and RT-qPCR analyses confirmed that FGE increased the protein expression of PI3K and phosphorylated AKT while suppressing GSK3β. Concurrently, FGE upregulated the transcription of key insulin secretion-related factors. By integrating these in vivo observations, we propose a clear inter-organ relationship. The bitter phytocompounds in FGE initially stimulate intestinal GLP-1 secretion via the TAS2R38 receptor. This circulating GLP-1 subsequently engages the pancreatic GLP-1R to activate the PI3K-AKT-GSK3β pathway, orchestrating both systemic appetite regulation and enhanced insulin sensitivity to restore metabolic homeostasis.

The chemical composition of fenugreek is highly complex and diverse. We previously systematically characterized the chemical constituents of FGE [34]. Although fenugreek contains multiple hypoglycemic constituents, the specific bitter ligands responsible for activating intestinal taste receptors have remained elusive. Building on this chemical characterization, the present study further investigated the compounds detectable in ileal tissues following FGE administration revealed the presence of several representative compounds detected in ileal tissues, including trigonelline, isoorientin, orientin, isovitexin, and dioscin [35–37]. These absorbed constituents likely represent the material basis underlying the intestinal pharmacological effects of FGE. Notably, trigonelline is a characteristic quality control marker of fenugreek in the Chinese Pharmacopoeia and has documented hypoglycemic activity, including the amelioration of IR in HepG2 cells [38]. Furthermore, trigonelline is a well-known contributor to the bitter taste profile of coffee [39]. These attributes position trigonelline as a highly plausible natural ligand capable of activating bitter taste receptors, prompting our subsequent structural and cellular investigations.

In the present study, a deliberate cross-species approach was employed. While our in vivo diabetic mice and in vitro STC-1 enteroendocrine cell experiments robustly investigated the murine ortholog (Tas2r138/TAS2R138) to establish physiological proof-of-concept, the computational molecular docking and MD simulations were purposefully performed using the human TAS2R38 receptor. This strategy was designed to bridge preclinical models with human clinical relevance. The murine TAS2R138 and human TAS2R38 orthologs share approximately 70% sequence homology, with highly conserved architectures in their transmembrane ligand-binding domains. Therefore, validating the structural binding affinity of trigonelline against the human TAS2R38 receptor critically underscores its potential translational value as a viable natural ligand for future human T2DM therapies.

TAS2R38 has been closely implicated in metabolic regulation [40], and databases such as the Human Protein Atlas confirm its widespread expression throughout the digestive system [41]. Previous studies have also demonstrated that TAS2R38 co-localizes with GLP-1-producing enteroendocrine L-cells [10]. However, precise structural information for extraoral TAS2Rs remains limited [42]. To bridge this gap, we conducted MD simulations using GROMACS to obtain a stable 3D conformation of TAS2R38. This optimized structure was subsequently utilized for molecular docking, a robust computational tool for predicting ligand-receptor binding affinities [43]. Generally, docking scores lower than −5.0 kcal/mol indicate strong binding interactions [44]. Our analysis revealed that most FGE-derived compounds identified in the ileum exhibited docking scores lower than −6.0 kcal/mol. Meanwhile, the MD simulation results of trigonelline and TAS2R38 show that a stable complex was formed. These computational results strongly suggest that FGE-derived compounds, particularly trigonelline, can act as putative structural ligands for TAS2R38. However, we acknowledge that computational docking serves primarily as a predictive structural hypothesis.

To experimentally validate these computational predictions, we utilized STC-1 enteroendocrine cells, a well-established in vitro model derived from mouse intestinal tissues that expresses TAS2R38 and the downstream incretin secretory machinery [11,45,46]. Treatment with trigonelline significantly triggered intracellular Ca^{2+} flux and GLP-1 secretion, definitively indicating the activation of bitter taste signaling. Furthermore, trigonelline robustly upregulated the transcription of the entire TAS2R38 signaling cascade, including *Tas2r138*, *Gnat3*, *Plcb2*, *Itpr3*, and *Trpm5*. Crucially, pharmacological blockade using the Gβγ inhibitor Gallein or the PLC inhibitor U73122 significantly abrogated the gene expression and signaling activation induced by trigonelline. These findings mechanistically confirm that trigonelline promotes GLP-1 secretion specifically via a Gβγ/PLC-dependent pathway.

Limitations and Future Directions

Despite these highly promising findings, we acknowledge several critical limitations in the present study that warrant further investigation to definitively establish the causal relationships within this gut-pancreas axis. First, regarding receptor specificity, while the pharmacological blockade using the Gβγ inhibitor Gallein and the PLC inhibitor U73122 successfully abrogated trigonelline-induced GLP-1 secretion in vitro, these inhibitors target downstream signaling nodes shared by multiple Gq-coupled GPCRs. The absence of specific Tas2r138 genetic knockdown/knockout models or highly specific receptor antagonists (coupled with a lack of inactive-inhibitor and established TAS2R38-agonist controls in our cell assays) precludes the definitive establishment of TAS2R138 as the exclusive target; our findings strongly implicate, but do not unequivocally prove, absolute receptor specificity. Future studies employing targeted receptor deletion are required to confirm these interactions. Second, computational docking models serve as predictive structural hypotheses and do not substitute for experimental receptor-binding assays. Third, while HE morphometry indicated improved overall islet area, rigorous insulin/glucagon co-staining and blinded morphometry are required in future studies to definitively quantify absolute β-cell mass changes. Fourth, while our in vivo data demonstrate concurrent intestinal GLP-1 release and pancreatic PI3K-AKT activation following FGE administration, this inter-organ communication remains fundamentally correlative. To construct an unassailable causal loop in vivo and definitively prove that the islet-protective effects of FGE are entirely dependent on intestinal GLP-1 release, future pharmacological blockade experiments utilizing specific GLP-1R antagonists, such as Exendin 9-39, or GLP-1R knockout murine models must be conducted.

5. Conclusions

In conclusion, the present study provides pharmacological evidence supporting the traditional medicinal application of FGE in the management of T2DM. Our findings elucidate a novel "gut-centric" pharmacological paradigm whereby FGE, driven by its bitter constituent trigonelline, restores glucolipid homeostasis primarily through the activation of a Gβγ/PLC-dependent signaling cascade, which is highly consistent with the involvement of the intestinal Tas2r138-mediated bitter taste signaling cascade. This localized receptor activation triggers the endogenous release of GLP-1, which subsequently engages the gut-pancreas axis to enhance pancreatic β-cell survival and insulin secretion via the PI3K-AKT-GSK3β pathway. Collectively, this comprehensive investigation provides profound molecular insights into the antidiabetic mechanisms of traditional bitter herbal medicines, establishing the physiological stimulation of extraoral bitter taste receptors as a viable, safe, and orally available strategy for metabolic disease intervention.

Supplementary Materials: The following supporting information can be downloaded at: https://www.mdpi.com/article/10.3390/cimb48111161/s1.

Author Contributions: H.N. conceived and designed the study, performed data analysis and interpretation, and drafted the manuscript. R.Y. conducted some experiments and processed the data. J.X. reviewed and revised the manuscript. L.C. and Y.N. participated in manuscript preparation. Z.P. conceived the study, provided funding support, and reviewed the manuscript. H.P. participated in the writing and critical revision of the manuscript. All authors have read and agreed to the published version of the manuscript.

Funding: This study was supported by the Postdoctoral Fellowship Program (Grade C) of the China Postdoctoral Science Foundation (Grant No. GZC20240076).

Institutional Review Board Statement: The animal experimental ethics for this study were approved by the Biological and Medical Ethics Review Committee of Minzu University of China (approval number: ECMUC2023005CAAA; Approval Date: 19 September 2023), and all procedures complied with the Guide for the Care and Use of Laboratory Animals.

Informed Consent Statement: Not applicable.

Data Availability Statement: The original contributions presented in this study are included in the article/supplementary material. Further inquiries can be directed to the corresponding author(s).

Acknowledgments: We gratefully acknowledge the Minzu University of China for providing the necessary equipment for this study.

Conflicts of Interest: The authors declare that they have no competing financial interests or personal relationships that could potentially influence the work reported in this paper.

References

1. Chen, F.; Wang, J.; He, S.; He, Y.; An, Y.; Gong, Q.; Chen, X.; Shuai, Y.; Wang, X.; Chen, Y.; et al. Influence of impaired glucose tolerance and type 2 diabetes on the multimorbidity cluster of cardiovascular disease and cancer: A post hoc analysis of the Da Qing Diabetes Prevention Outcome Study. *BMC Med*. **2024**, *22*, 534. [CrossRef] [PubMed]
2. Wang, X.; Tian, R.; Liang, C.; Jia, Y.; Zhao, L.; Xie, Q.; Huang, F.; Yuan, H. Biomimetic nanoplatform with microbiome modulation and antioxidant functions ameliorating insulin resistance and pancreatic beta-cell dysfunction for T2DM management. *Biomaterials* **2025**, *313*, 122804. [CrossRef] [PubMed]
3. Eizirik, D.L.; Pasquali, L.; Cnop, M. Pancreatic beta-cells in type 1 and type 2 diabetes mellitus: Different pathways to failure. *Nat. Rev. Endocrinol*. **2020**, *16*, 349–362. [CrossRef] [PubMed]
4. Drucker, D.J. Mechanisms of Action and Therapeutic Application of Glucagon-like Peptide-1. *Cell Metab*. **2018**, *27*, 740–756. [CrossRef] [PubMed]
5. Du, Y.; Bai, L.; Fan, B.; Ding, H.; Ding, H.; Hou, L.; Ma, H.; Xing, N.; Wang, F. Effect of SGLT2 inhibitors versus DPP4 inhibitors or GLP-1 agonists on diabetic foot-related extremity amputation in patients with T2DM: A meta-analysis. *Prim. Care Diabetes* **2022**, *16*, 156–161. [CrossRef] [PubMed]

6. Reiss, A.B.; Gulkarov, S.; Lau, R.; Klek, S.P.; Srivastava, A.; Renna, H.A.; De Leon, J. Weight Reduction with GLP-1 Agonists and Paths for Discontinuation While Maintaining Weight Loss. *Biomolecules* **2025**, *15*, 408. [CrossRef] [PubMed]
7. Rosenstock, J.; Frias, J.; Jastreboff, A.M.; Du, Y.; Lou, J.; Gurbuz, S.; Thomas, M.K.; Hartman, M.L.; Haupt, A.; Milicevic, Z.; et al. Retatrutide, a GIP, GLP-1 and glucagon receptor agonist, for people with type 2 diabetes: A randomised, double-blind, placebo and active-controlled, parallel-group, phase 2 trial conducted in the USA. *Lancet* **2023**, *402*, 529–544. [CrossRef] [PubMed]
8. Lee, S.H.; Ko, H.M.; Jee, W.; Kim, H.; Chung, W.S.; Jang, H.J. Isosinensetin Stimulates Glucagon-like Peptide-1 Secretion via Activation of hTAS2R50 and the G(betagamma)-Mediated Signaling Pathway. *Int. J. Mol. Sci.* **2023**, *24*, 3682. [CrossRef] [PubMed]
9. Noya-Leal, F.; van der Wielen, N.; Behrens, M.; Rouschop, S.; van Arkel, J.; Jongsma, M.; Witkamp, R.; Mes, J.J.; Bastiaan-Net, S.; Meijerink, J. Rebaudioside A from Stevia rebaudiana stimulates GLP-1 release by enteroendocrine cells via bitter taste signalling pathways. *Food Funct.* **2023**, *14*, 6914–6928. [CrossRef] [PubMed]
10. Chou, W.L. Therapeutic potential of targeting intestinal bitter taste receptors in diabetes associated with dyslipidemia. *Pharmacol. Res.* **2021**, *170*, 105693. [CrossRef] [PubMed]
11. Yue, X.; Liang, J.; Gu, F.; Du, D.; Chen, F. Berberine activates bitter taste responses of enteroendocrine STC-1 cells. *Mol. Cell Biochem.* **2018**, *447*, 21–32. [CrossRef] [PubMed]
12. Chen, M.C.; Wu, S.V.; Reeve, J.R. Bitter stimuli induce Ca2+ signaling and CCK release in enteroendocrine STC-1 cells: Role of L-type voltage-sensitive Ca2+ channels. *Am. J. Physiol. Cell Physiol.* **2006**, *291*, C726. [CrossRef]
13. Kim, J.; Noh, W.; Kim, A.; Choi, Y.; Kim, Y.S. The Effect of Fenugreek in Type 2 Diabetes and Prediabetes: A Systematic Review and Meta-Analysis of Randomized Controlled Trials. *Int. J. Mol. Sci.* **2023**, *24*, 13999. [CrossRef] [PubMed]
14. Gong, J.; Fang, K.; Dong, H.; Wang, D.; Hu, M.; Lu, F. Effect of fenugreek on hyperglycaemia and hyperlipidemia in diabetes and prediabetes: A meta-analysis. *J. Ethnopharmacol.* **2016**, *194*, 260–268. [CrossRef] [PubMed]
15. Hamden, K.; Bengara, A.; Amri, Z.; Elfeki, A. Experimental diabetes treated with trigonelline: Effect on key enzymes related to diabetes and hypertension, beta-cell and liver function. *Mol. Cell Biochem.* **2013**, *381*, 85–94. [CrossRef] [PubMed]
16. Wang, Y.; Wang, A.; Alkhalidy, H.; Luo, J.; Moomaw, E.; Neilson, A.P.; Liu, D. Flavone Hispidulin Stimulates Glucagon-Like Peptide-1 Secretion and Ameliorates Hyperglycemia in Streptozotocin-Induced Diabetic Mice. *Mol. Nutr. Food Res.* **2020**, *64*, e1900978. [CrossRef] [PubMed]
17. Sarker, D.K.; Ray, P.; Dutta, A.K.; Rouf, R.; Uddin, S.J. Antidiabetic potential of fenugreek (Trigonella foenum-graecum): A magic herb for diabetes mellitus. *Food Sci. Nutr.* **2024**, *12*, 7108–7136. [CrossRef] [PubMed]
18. Shao, W.; Xiao, C.; Yong, T.; Zhang, Y.; Hu, H.; Xie, T.; Liu, R.; Huang, L.; Li, X.; Xie, Y.; et al. A polysaccharide isolated from Ganoderma lucidum ameliorates hyperglycemia through modulating gut microbiota in type 2 diabetic mice. *Int. J. Biol. Macromol.* **2022**, *197*, 23–38. [CrossRef] [PubMed]
19. Li, P.; Fan, C.; Cai, Y.; Fang, S.; Zeng, Y.; Zhang, Y.; Lin, X.; Zhang, H.; Xue, Y.; Guan, M. Transplantation of brown adipose tissue up-regulates miR-99a to ameliorate liver metabolic disorders in diabetic mice by targeting NOX4. *Adipocyte* **2020**, *9*, 57–67. [CrossRef] [PubMed]
20. Zhang, L.; Zhou, X.; Chen, H.; You, L.; Zhang, T.; Cheng, M.; Yao, Y.; Pan, X.; Yang, X. Mulberry extract ameliorates T2DM-related symptoms via AMPK pathway in STZ-HFD-induced C57BL/6J mice. *J. Ethnopharmacol.* **2023**, *313*, 116475. [CrossRef] [PubMed]
21. Luo, W.; Deng, J.; He, J.; Yin, L.; You, R.; Zhang, L.; Shen, J.; Han, Z.; Xie, F.; He, J.; et al. Integration of molecular docking, molecular dynamics and network pharmacology to explore the multi-target pharmacology of fenugreek against diabetes. *J. Cell Mol. Med.* **2023**, *27*, 1959–1974. [CrossRef] [PubMed]
22. Chi, L.; Niu, H.; Niu, Y.; Yao, R.; Shi, D.; Lu, B.; Pang, Z. Trigonella foenum-graecum L. ameliorates metabolism-associated fatty liver disease in type 2 diabetic mice: A multi-omics mechanism analysis. *J. Ethnopharmacol.* **2025**, *348*, 119862. [CrossRef] [PubMed]
23. Chaturvedi, U.; Shrivastava, A.; Bhadauria, S.; Saxena, J.K.; Bhatia, G. A mechanism-based pharmacological evaluation of efficacy of Trigonella foenum graecum (fenugreek) seeds in regulation of dyslipidemia and oxidative stress in hyperlipidemic rats. *J. Cardiovasc. Pharmacol.* **2013**, *61*, 505–512. [CrossRef] [PubMed]
24. Askarpour, M.; Alami, F.; Campbell, M.S.; Venkatakrishnan, K.; Hadi, A.; Ghaedi, E. Effect of fenugreek supplementation on blood lipids and body weight: A systematic review and meta-analysis of randomized controlled trials. *J. Ethnopharmacol.* **2020**, *253*, 112538. [CrossRef] [PubMed]
25. Li, J.; Xu, J.; Hou, R.; Jin, X.; Wang, J.; Yang, N.; Yang, L.; Liu, L.; Tao, F.; Lu, H. Qing-Hua Granule induces GLP-1 secretion via bitter taste receptor in db/db mice. *Biomed. Pharmacother.* **2017**, *89*, 10–17. [CrossRef] [PubMed]
26. Prandi, S.; Voigt, A.; Meyerhof, W.; Behrens, M. Expression profiling of Tas2r genes reveals a complex pattern along the mouse GI tract and the presence of Tas2r131 in a subset of intestinal Paneth cells. *Cell Mol. Life Sci.* **2018**, *75*, 49–65. [CrossRef] [PubMed]
27. Jalsevac, F.; Segu, H.; Balaguer, F.; Ocana, T.; Moreira, R.; Abad-Jorda, L.; Gracia-Sancho, J.; Fernandez-Iglesias, A.; Andres-Lacueva, C.; Martinez-Huelamo, M.; et al. TAS2R5 and TAS2R38 are bitter taste receptors whose colonic expressions could play important roles in age-associated processes. *J. Nutr. Biochem.* **2025**, *140*, 109872. [CrossRef] [PubMed]

28. Bertran, L.; Portillo-Carrasquer, M.; Martinez, S.; Aguilar, C.; Lopez-Dupla, M.; Riesco, D.; Binetti, J.; Vives, M.; Sabench, F.; Del Castillo, D.; et al. Expression of Jejunal Taste Receptors in Women with Morbid Obesity. *Nutrients* **2021**, *13*, 2437. [CrossRef] [PubMed]
29. Marzook, A.; Tomas, A.; Jones, B. The Interplay of Glucagon-Like Peptide-1 Receptor Trafficking and Signalling in Pancreatic Beta Cells. *Front Endocrinol (Lausanne)* **2021**, 678055. [CrossRef]
30. Zaimia, N.; Obeid, J.; Varrault, A.; Sabatier, J.; Broca, C.; Gilon, P.; Costes, S.; Bertrand, G.; Ravier, M.A. GLP-1 and GIP receptors signal through distinct beta-arrestin 2-dependent pathways to regulate pancreatic beta cell function. *Cell Rep.* **2023**, *42*, 113326. [CrossRef] [PubMed]
31. Huang, C.; Yuan, L.; Cao, S. Endogenous GLP-1 as a key self-defense molecule against lipotoxicity in pancreatic islets. *Int. J. Mol. Med.* **2015**, *36*, 173–185. [CrossRef] [PubMed]
32. Holter, M.M.; Saikia, M.; Cummings, B.P. Alpha-cell paracrine signaling in the regulation of beta-cell insulin secretion. *Front. Endocrinol.* **2022**, *13*, 934775. [CrossRef] [PubMed]
33. Cheng, Z.; Guo, D.; Ruzi, A.; Pan, T.; You, K.; Chen, Y.; Huang, X.; Zhang, J.; Yang, F.; Niu, L.; et al. Modeling MEN1 with Patient-Origin iPSCs Reveals GLP-1R Mediated Hypersecretion of Insulin. *Cells* **2022**, *11*, 2387. [CrossRef] [PubMed]
34. Niu, Y.; Niu, H.; Chi, L.; Li, P.; Du, J.; Wang, X.; He, X.; Lu, B.; Pang, Z. Trigonella foenum-graecum L. protects against renal function decline in a mouse model of type 2 diabetic nephropathy by modulating the PI3K-Akt-ERK signaling pathway. *Front. Pharmacol.* **2025**, *16*, 1566723. [CrossRef] [PubMed]
35. Alipour, S.; Mirfardi, A.; Seradj, S.H.; Mohammadi, R.; Masjedi, M. Trigonella foenum-graecum L. (fenugreek) seed extract-loaded niosomal thin film as a wound dressing: Formulation, optimisation, in vitro and in vivo characterisation. *Nat. Prod. Res.* **2025**, *40*, 5395–5403. [CrossRef] [PubMed]
36. Khoja, K.K.; Howes, M.R.; Hider, R.; Sharp, P.A.; Farrell, I.W.; Latunde-Dada, G.O. Cytotoxicity of Fenugreek Sprout and Seed Extracts and Their Bioactive Constituents on MCF-7 Breast Cancer Cells. *Nutrients* **2022**, *14*, 784. [CrossRef] [PubMed]
37. Singh, P.; Bajpai, V.; Gond, V.; Kumar, A.; Tadigoppula, N.; Kumar, B. Determination of Bioactive Compounds of Fenugreek (Trigonella foenum-graecum) Seeds Using LC-MS Techniques. *Methods Mol. Biol.* **2020**, *2107*, 377–393. [CrossRef] [PubMed]
38. Sharma, L.; Lone, N.A.; Knott, R.M.; Hassan, A.; Abdullah, T. Trigonelline prevents high cholesterol and high fat diet induced hepatic lipid accumulation and lipo-toxicity in C57BL/6J mice, via restoration of hepatic autophagy. *Food Chem. Toxicol.* **2018**, *121*, 283–296. [CrossRef] [PubMed]
39. Atlabachew, M.; Abebe, A.; Alemneh Wubieneh, T.; Tefera Habtemariam, Y. Rapid and simultaneous determination of trigonelline, caffeine, and chlorogenic acid in green coffee bean extract. *Food Sci. Nutr.* **2021**, *9*, 5028–5035. [CrossRef] [PubMed]
40. Jeruzal-Swiatecka, J.; Fendler, W.; Pietruszewska, W. Clinical Role of Extraoral Bitter Taste Receptors. *Int. J. Mol. Sci.* **2020**, *21*, 5156. [CrossRef] [PubMed]
41. Robino, A.; Rosso, N.; Guerra, M.; Corleone, P.; Casagranda, B.; Giraudi, P.J.; Tiribelli, C.; Simeth, C.; Monica, F.; La Bianca, M.; et al. Taste perception and expression in stomach of bitter taste receptor tas2r38 in obese and lean subjects. *Appetite* **2021**, *166*, 105595. [CrossRef] [PubMed]
42. Xu, W.; Wu, L.; Liu, S.; Liu, X.; Cao, X.; Zhou, C.; Zhang, J.; Fu, Y.; Guo, Y.; Wu, Y.; et al. Structural basis for strychnine activation of human bitter taste receptor TAS2R46. *Science* **2022**, *377*, 1298–1304. [CrossRef] [PubMed]
43. Gupta, M.; Sharma, R.; Kumar, A. Docking techniques in pharmacology: How much promising? *Comput. Biol. Chem.* **2018**, *76*, 210–217. [CrossRef] [PubMed]
44. Niu, H.; Fan, L.; Zhao, L.; Yao, R.; He, X.; Lu, B.; Pang, Z. The therapeutic mechanism of PuRenDan for the treatment of diabetic nephropathy: Network pharmacology and experimental verification. *J. Ethnopharmacol.* **2022**, *293*, 115283. [CrossRef] [PubMed]
45. Qi, L.; Shuai, T.; Da, J.; Ezra, B.; Luis, S.D. In-vitro GLP-1 Release Assay Using STC-1 Cells. *Bio-Protocol* **2020**, *10*, e3717. [CrossRef] [PubMed]
46. Su, W.; Li, Y.; Chang, A.K.; Sheng, T.; Pei, Y.; Li, J.; Li, H.; Liu, K.; Xu, L.; Liu, W.; et al. Identification of Novel Alkaloids from Portulaca oleracea L. and Characterization of Their Pharmacokinetics and GLP-1 Secretion-Promoting Activity in STC-1 Cells. *J. Agric. Food Chem.* **2023**, *71*, 19804–19816. [CrossRef] [PubMed]

Disclaimer/Publisher's Note: The statements, opinions and data contained in all publications are solely those of the individual author(s) and contributor(s) and not of MDPI and/or the editor(s). MDPI and/or the editor(s) disclaim responsibility for any injury to people or property resulting from any ideas, methods, instructions or products referred to in the content.